



**University of
Zurich**^{UZH}

**Zurich Open Repository and
Archive**

University of Zurich
University Library
Strickhofstrasse 39
CH-8057 Zurich
www.zora.uzh.ch

Year: 2014

**Multi-isotope labeling (^{13}C , ^{18}O , ^2H) of fresh assimilates to trace organic matter
dynamics in the plant-soil system**

Studer, Mirjam S ; Siegwolf, R T W ; Leuenberger, M ; Abiven, Samuel

DOI: <https://doi.org/10.5194/bgd-11-15911-2014>

Posted at the Zurich Open Repository and Archive, University of Zurich

ZORA URL: <https://doi.org/10.5167/uzh-101444>

Journal Article

Accepted Version

Originally published at:

Studer, Mirjam S; Siegwolf, R T W; Leuenberger, M; Abiven, Samuel (2014). Multi-isotope labeling (^{13}C , ^{18}O , ^2H) of fresh assimilates to trace organic matter dynamics in the plant-soil system. *Biogeosciences Discussions*, 11:15911-15943.

DOI: <https://doi.org/10.5194/bgd-11-15911-2014>

1 **Multi-isotope labelling (^{13}C , ^{18}O , ^2H) of fresh**
2 **assimilates to trace organic matter dynamics in the**
3 **plant-soil system**

4 **M. S. Studer^{1,2}, R. T. W. Siegwolf², M. Leuenberger³, S. Abiven¹**

5 [1] Department of Geography, University of Zurich, Winterthurerstr. 190, 8057
6 Zurich, Switzerland

7 [2] Laboratory of Atmospheric Chemistry, Paul Scherrer Institute, 5232 Villigen PSI,
8 Switzerland

9 [3] Climate and Environmental Physics, Physics Institute and Oeschger Centre for
10 Climate Change Research, University of Bern, Sidlerstr. 5, 3012 Bern

11 Correspondence to: Dr. S. Abiven (samuel.abiven@geo.uzh.ch)

12 **Abstract**

13 Isotope labelling is a powerful tool to study elemental cycling within terrestrial
14 ecosystems. Here we describe a new multi-isotope technique to label organic matter
15 (OM).

16 We exposed poplars (*Populus deltoides x nigra*) for 14 days to an atmosphere
17 enriched in $^{13}\text{CO}_2$ and depleted in $^2\text{H}_2^{18}\text{O}$. After one week, the water-soluble leaf OM
18 ($\delta^{13}\text{C} = 1346 \pm 162 \text{ ‰}$) and the leaf water were strongly labelled ($\delta^{18}\text{O} = -63 \pm 8 \text{ ‰}$,
19 $\delta^2\text{H} = -156 \pm 15 \text{ ‰}$). The leaf water isotopic composition was between the
20 atmospheric and stem water, indicating a considerable diffusion of vapour into the
21 leaves (58 - 69 %). The atomic ratios of the labels recovered ($^{18}\text{O}/^{13}\text{C}$, $^2\text{H}/^{13}\text{C}$) were 2
22 - 4 times higher in leaves than in the stems and roots. This either indicates the
23 synthesis of more condensed compounds (lignin vs. cellulose) in roots and stems, or
24 be the result of O and H exchange and fractionation processes during transport and
25 biosynthesis.

26 We demonstrate that the three major OM elements (C, O, H) can be labelled and
27 traced simultaneously within the plant. This approach could be of interdisciplinary
28 interest for the fields of plant physiology, paleoclimatic reconstruction or soil science.

29

30 **1 Introduction**

31 Artificial labelling with stable isotopes facilitates the observation of bio(geo)chemical
32 cycling of elements or compounds with minor disturbance to the plant-soil systems. It
33 has provided many insights into plant carbon allocation patterns (e.g. Simard et al.
34 1997; Keel et al. 2006; Högberg et al. 2008), water dynamics (e.g. in Plamboeck et al.
35 2007; Kulmatiski et al. 2010) and soil organic matter processes (e.g. in Bird and Torn
36 2006; Girardin et al. 2009) in terrestrial ecosystems. Only a few studies used labelling
37 approaches with more than one stable isotope, for example to study the interactions
38 between the carbon and nitrogen cycle (e.g. in Bird and Torn 2006; Schenck zu
39 Schweinsberg-Mickan et al. 2010). However, to our knowledge isotopic labelling of
40 organic matter (OM) with its three major elements, carbon (C), oxygen (O) and
41 hydrogen (H), has never been done in ecosystem studies before, even though
42 combined $\delta^{13}\text{C}$, $\delta^{18}\text{O}$ and $\delta^2\text{H}$ analyses have been widely used to study plant
43 physiological processes and to reconstruct past climatic conditions (Hangartner et al.,
44 2012; Roden and Farquhar, 2012; Scheidegger et al., 2000; Werner et al., 2012).
45 Similarly, an artificial labelling with those isotopes would be useful to clarify basic
46 mechanisms related to the plant water-use efficiency or the oxygen and hydrogen
47 signals in tree rings, but also to study other OM dynamics in the plant-soil system
48 such as OM decomposition in the soil.

49 The C, O and H contents of organic matter have been applied to distinguish major
50 groups of compounds, by plotting the atomic ratios O/C and H/C in a van Krevelen
51 diagram (Kim et al., 2003; Ohno et al., 2010; Sleighter and Hatcher, 2007). This
52 approach is based on the distinct molecular formula of organic compounds. For
53 example the glucose molecule ($\text{C}_6\text{H}_{12}\text{O}_6$) is characterized by high O/C (= 1) and H/C
54 (= 2) ratios and is the precursor of other compounds, such as cellulose ($(\text{C}_6\text{H}_{10}\text{O}_5)_n$)
55 (O/C = 0.8, H/C = 1.7). Condensation or reduction reactions during biosynthesis lead
56 to other compound groups with lower atomic ratios (e.g. lignin) or similar H/C, but
57 lower O/C ratios (e.g. lipids, proteins) compared to glucose. Following the logic of
58 the van Krevelen diagram, we wanted to test, if we can use the isotopic ratios $^{18}\text{O}/^{13}\text{C}$
59 and $^2\text{H}/^{13}\text{C}$ of the labels recovered in plant-soil bulk materials after labelling the fresh
60 assimilates with those stable isotopes, to detect the utilization of the assimilates for
61 the synthesis of different OM compounds. With this multi-labelling approach we
62 would gain information of high specificity of the characteristics of the OM formed by
63 simple isotopic analysis of bulk material. This has several advantages compared to

64 common compound specific analysis, such as being much less laborious and less
65 expensive and yield integrated information on the plant-soil compartments sampled.
66 In this study we added the ^{13}C , ^{18}O and ^2H labels via the gaseous phase in the plants'
67 atmosphere (CO_2 , water vapour). Pre-grown plants were exposed to the labelled
68 atmosphere continuously for fourteen days under laboratory conditions and the labels
69 added were traced in different plant-soil compartments (leaves, petioles, stems,
70 cuttings, roots, soil organic matter) and at different points in time. We applied a
71 simple isotope mixing model to estimate the fraction of ^{18}O and ^2H that entered the
72 leaf by diffusion from the atmosphere into the leaf intercellular cavities and plotted
73 the atomic and isotopic ratios of the OM formed in van Krevelen diagrams to test if
74 the multi-isotope labelling approach can be used to detect changes in the OM
75 characteristics.

76 **2 Material and Methods**

77 **2.1 Plants and soil**

78 The soil (cambisol) was sampled from the upper 15 cm in a beech forest ($8^\circ 33' \text{ E}$, 47°
79 $23' \text{ N}$, 500 m elevation), coarse sieved (2.5 x 3.5 cm) and large pieces of hardly
80 decomposed organic material were removed. The soil had a clay loam texture, a pH of
81 4.8, an organic C content of 2.8 % and a C/N ratio of 11. The plant pots (volume = 8.2
82 dm^3) were filled with $3018 \pm 177 \text{ g}$ soil (dry weight equivalent). 15 Poplar seedlings
83 (*Populus deltoides x nigra*, Dorskamp clone) were grown indoors from 20 cm long
84 stem cuttings for five weeks before they were transferred into labelling chambers
85 (described below). They were kept in the chamber for acclimatization for one week
86 prior to labelling. At the beginning of the labelling experiments, the average dry
87 weight of fresh plant biomass (without the wooden stem cutting) was $3.3 \pm 0.1 \text{ g}$ and
88 the average total leaf area was $641 \pm 6 \text{ cm}^2$ per plant. At the end of the experiment
89 (last sampling) the dry weight was $5.4 \pm 1.1 \text{ g}$ and the total leaf area was 1354 ± 161
90 cm^2 , respectively. The leaf area was measured with a handheld area meter (CID-203
91 Laser leaf area meter, CID Inc.).

92 **2.2 Labelling chamber, procedure and environmental conditions**

93 The labelling chambers (MICE - Multi-Isotope labelling in a Controlled Environment
94 - facility) provide a hermetical separation of the shoots from the roots, rhizosphere
95 and soil. The plant shoots are enclosed by one large polycarbonate box (volume 1.2

96 m³) with a removable front plate and five 2 cm wide gaps in the bottom plate to slide
97 in three plants in each row. Small polycarbonate pieces, Kapton tape and a malleable
98 sealant (Terostat IX, Henkel AG & Co.) wrapped around the stem cuttings were used
99 to seal off the upper from the lower chamber. Environmental chamber conditions are
100 automatically controlled (CO₂ and H₂O concentration, light) and monitored (CO₂ and
101 H₂O concentration, air temperature and pressure) every 5 seconds. The belowground
102 compartments (soil and roots) are in fifteen individual pots, which are hermetically
103 sealed and aerated. This setup ensures that all plants receive the same labelling
104 treatment and prevents the diffusion of labelled atmospheric gases into the soil.
105 The isotope labels (¹³C, ¹⁸O and ²H) were added continuously for 14 days via gaseous
106 phase to the plant shoots. We used CO₂ enriched in ¹³C (10 atom% ¹³C-CO₂,
107 Cambridge Isotope Laboratories, Inc.), and water vapour depleted in ¹⁸O and ²H ($\delta^{18}\text{O}$
108 = - 370 ‰ and $\delta^2\text{H}$ = - 813 ‰, waste product from enrichment columns at the Paul
109 Scherrer Institute). Thus the labelled gases added were enriched by 8.90 atom% ¹³C
110 and depleted by 0.07 atom% ¹⁸O and 0.01 atom% ²H relative to the ambient air.
111 The environmental conditions in the labelling chambers were set to promote the water
112 vapour label uptake via leaves. The soil moisture was maintained at 100 % field
113 capacity and the relative air humidity was 74 %. The light intensity was low (80 ± 25
114 $\mu\text{mol m}^{-2} \text{s}^{-1}$ photosynthetic active radiation), and the CO₂ concentration was kept at
115 508 ± 22 ppm in order to maintain a high atmospheric carbon supply. The day-night
116 cycles were twelve hours and the temperature within the labelling chamber was 31 ± 3
117 °C throughout the experiments.

118 **2.3 Sample collection**

119 The plant-soil systems were destructively harvested at five sampling dates (three
120 replicates each) to detect the dynamics of the labelling over time, which was of
121 special importance to compare the pulse with continuous ¹³CO₂ labelling techniques
122 that was performed in parallel to this study (Studer et al., 2014). The first sampling
123 was done one day before the labelling experiment started (unlabelled control, referred
124 to as t = 0). Subsequently plant-soil systems were sampled after 1, 2, 8 and 14 days of
125 continuous labelling.

126 At each sampling date the plant-soil systems were separated into leaves, petioles,
127 stems, cuttings, roots (washed with deionised water and carefully dabbed with tissue)
128 and bulk soil (visible roots were removed with tweezers). The leaves (sub-sample of

129 six leaves) were sampled all along the stem (homogeneously distributed). The
130 uppermost leaves, newly formed during the experiment (completely labelled), were
131 excluded, since we wanted to study the tracer uptake and translocation dynamics in
132 already existing leaves prior to the treatment. Note that this procedure is the reason
133 for the distinct values reported for the ^{13}C in leaves and petioles in this study and in
134 Studer et al. (2014), since we analysed in the latter not only a sub-sample, but the total
135 leaf and petiole bulk material (including freshly produced leaves) to assess the ^{13}C
136 budget. In one out of the three plant replicates we took two leaf sub-samples from
137 distinct positions along the shoot. We sampled six leaves from the upper and six
138 leaves from the lower half of the shoot (thereafter referred to as "top" and "bottom",
139 respectively). Leaves, stems, roots and bulk soil were collected in airtight glass vials
140 and frozen immediately at $-20\text{ }^{\circ}\text{C}$ for later cryogenic vacuum extraction of the tissue
141 water. Cuttings and petioles were dried for 24 hours at $60\text{ }^{\circ}\text{C}$.

142 The tissue water was extracted with cryogenic vacuum extraction by heating the
143 frozen samples within the sampling vials in a water bath at $80\text{ }^{\circ}\text{C}$ under a vacuum
144 (10^{-3} mbar) for two hours. The evaporating water was collected in U-vials submersed
145 in a liquid nitrogen cold trap. After thawing (within the closed U-vials), the water
146 samples were transferred into vials and stored frozen at $-20\text{ }^{\circ}\text{C}$ for later $\delta^{18}\text{O}$ and $\delta^2\text{H}$
147 analysis. To study the water dynamics, additional water vapour samples from the
148 chamber air were collected by peltier-cooled water condensers (in an external air
149 circuit connected to the plant labelling chamber) and analysed for $\delta^{18}\text{O}$ and $\delta^2\text{H}$.

150 The dried plant residues of the cryogenic vacuum extraction were used for isotopic
151 bulk analyses (described below). The leaf water-soluble organic matter was extracted
152 by hot water extraction. 60 mg milled leaf material was dissolved in 1.5 ml of
153 deionised water and heated in a water bath ($85\text{ }^{\circ}\text{C}$) for 30 min. After cooling and
154 centrifugation ($10'000\text{ g}$, 2 min), the supernatant was freeze-dried and analysed for
155 $\delta^{13}\text{C}$. $\delta^2\text{H}$ analyses were not possible on the hot water extracts (mainly sugars), due to
156 incomplete equilibration with ambient water vapour (Filot, 2010).

157 **2.4 Isotopic and elemental analyses**

158 All samples were milled to a fine powder with a steel ball mill and weighed into tin
159 ($\delta^{13}\text{C}$ analyses) or silver ($\delta^{18}\text{O}$ and $\delta^2\text{H}$ analyses) capsules and measured by isotope-
160 ratio mass spectrometry (IRMS). The $\delta^{13}\text{C}$ samples were combusted in an elemental
161 analyser (EA 1110, Carlo Erba) and the resulting CO_2 was transferred in a helium

162 stream via a variable open-split interface (ConFlo II, Finnigan MAT) to the IRMS
163 (Delta S, Thermo Finnigan; see Werner et al. 1999). The samples for $\delta^{18}\text{O}$ analyses
164 were pyrolysed in an elemental analyser (EA 1108, Carlo Erba) and transferred via
165 ConFlo III interface (Thermo Finnigan) to the IRMS (Delta plus XL, Thermo
166 Finnigan). The samples for $\delta^2\text{H}$ analyses were equilibrated with water vapour of
167 known a signature prior to the IRMS measurements, to determine the isotopic
168 signature of the non-exchangeable hydrogen (as described in Filot et al. 2006;
169 Hangartner et al. 2012). After equilibration the samples were pyrolysed in a
170 thermochemical elemental analyser (TC/EA, Thermo-Finnigan) at a temperature of
171 1425 °C and the gaseous products were carried by a helium stream via a ConFlow II
172 open split interface (Thermo Finnigan) into the IRMS (Isoprime, Cheadle). The
173 measurement of leaf, stem and root tissue was repeated with plant material of
174 sampling date $t = 0$, using depleted water vapour to equilibrate the samples, in order
175 to estimate the amount of exchangeable hydrogen (and oxygen). The measurement
176 precisions of the solid sample analyses, assessed by working standards measured
177 frequently along with the experimental samples, were 0.12 ‰ $\delta^{13}\text{C}$, 0.54 ‰ $\delta^{18}\text{O}$ and
178 1 ‰ $\delta^2\text{H}$. The sample precisions are lower than reported for measurements of natural
179 abundance, since highly labelled sample material was analysed.

180 Elemental C, H and N content of solid samples was analysed in an elemental analyzer
181 (CHN-900, Leco Corp.) and the elemental O content by RO-478 (Leco Corp.).

182 The liquid samples from the cryogenic vacuum extraction (tissue water) were
183 pyrolysed in an elemental analyser (TC/EA, Thermo Finnigan) and the evolving CO
184 and H₂ gases were transferred via the ConFlo III interface (Thermo Finnigan) to a
185 IRMS (Delta plus XL, Thermo Finnigan) for oxygen and hydrogen isotope ratio
186 analysis (Gehre et al., 2004). The precision of the liquid sample measurement was \pm
187 0.75 ‰ $\delta^{18}\text{O}$ and \pm 1.59 ‰ $\delta^2\text{H}$.

188 **2.5 Calculations**

189 Isotopic ratios were expressed in delta (δ) notation as the deviation (in ‰) from the
190 international standards Vienna Pee Dee Belemnite (V-PDB, $^{13}\text{C}/^{12}\text{C} = 1.11802 \times 10^{-2}$)
191 and Vienna Standard Mean Ocean Water (V-SMOW, $^{18}\text{O}/^{16}\text{O} = 2.0052 \times 10^{-3}$ and
192 $^2\text{H}/^1\text{H} = 1.5575 \times 10^{-4}$). The significance of changes in isotopic signature between the
193 sampling dates and the unlabelled control ($t = 0$) were statistically tested by t-tests
194 performed by R software (R Core Team 2014).

195 In the following paragraphs we describe first the calculations for the leaf water source
 196 partitioning (Eqn 1 - 4). These equations are given for the oxygen isotope (^{18}O), but
 197 they apply also for hydrogen (^2H). The calculations for the relative recovery of the
 198 three isotopes ($^{18}\text{O}/^{13}\text{C}$ and $^2\text{H}/^{13}\text{C}$) in the bulk organic matter are described (Eqn 5 -
 199 7).

200 The leaf water isotopic signature (at steady state) can be described by a model of
 201 Dongmann et al. (1974) to calculate leaf water H_2^{18}O enrichment, a derivative of
 202 Craig & Gordon (1965) (Eqn 1). According to this model, the isotopic signature of the
 203 leaf water (L) is the result of kinetic (ϵ^k) and equilibrium (ϵ^*) fractionation processes
 204 during evaporation of the source water (S) within the leaves and the back-diffusion of
 205 atmospheric water vapour (V) into the leaves as affected by relative air humidity (h).

$$206 \quad \delta^{18}\text{O}_L = \delta^{18}\text{O}_S + \epsilon^k + \epsilon^* + (\delta^{18}\text{O}_V - \delta^{18}\text{O}_S - \epsilon^k) \cdot h \quad \text{Eqn 1}$$

207 We used a two-source isotope mixing model (Eqn 2, principles described in Dawson
 208 et al. 2002) to assess the contribution of the two main water pools (soil and
 209 atmospheric water) to the leaf water based on its isotopic signatures. An overview on
 210 the input data for the mixing model is given as in Appendix A (Fig. A1).

$$211 \quad f_{\text{source},2} = \frac{\delta^{18}\text{O}_{\text{leaf},\text{water}} - \delta^{18}\text{O}_{\text{source},1}}{\delta^{18}\text{O}_{\text{source},2} - \delta^{18}\text{O}_{\text{source},1}} \quad \text{Eqn 2}$$

212 , where $\delta^{18}\text{O}_{\text{leaf},\text{water}}$ is the isotopic signature (in ‰) of water extracted from the leaves
 213 at a specific sampling date and $\delta^{18}\text{O}_{\text{source},1}$ and $\delta^{18}\text{O}_{\text{source},2}$ are the theoretical isotopic
 214 signatures of the leaf water if all water would originate either from the soil (source 1)
 215 or the atmospheric (source 2) water pool.

216 The first source, thereafter referred to as "evaporating source", represents the water
 217 taken up from the soil by the roots, which is transported via the xylem to the leaf,
 218 where it evaporates. The isotopic signature of the evaporating source (Eqn 3) is
 219 estimated by the maximum leaf water enrichment that would occur at 0 % relative air
 220 humidity i.e. by the first part of the Dongmann approach (solving Eqn 1 with $h = 0$).

$$221 \quad \delta^{18}\text{O}_{\text{source},1} = \delta^{18}\text{O}_{\text{stem},\text{water}} + \epsilon^k + \epsilon^*_{\text{atm}} \quad \text{Eqn 3}$$

222 , where $\delta^{18}\text{O}_{\text{stem},\text{water}}$ is the isotopic signature (in ‰) of the water extracted from the
 223 stem tissue (approximating the xylem water) and ϵ^k and ϵ^*_{atm} are the kinetic and
 224 equilibrium fractionation terms, respectively, at the specific sampling date.

225 The second source, thereafter called "condensation source", refers to the water vapour
 226 that diffuses from the atmosphere into the leaves and condensates at the cell walls.
 227 The contribution of this source would be maximal at 100 % relative humidity, which
 228 results in Eqn 4 when solving Eqn 1 with $h = 1$.

$$229 \quad \delta^{18}\text{O}_{source,2} = \delta^{18}\text{O}_{atm,vap} + \varepsilon_{atm}^* = \delta^{18}\text{O}_{atm,cond} - \varepsilon_{pelt}^* + \varepsilon_{atm}^* \quad \text{Eqn 4}$$

230 , where $\delta^{18}\text{O}_{atm,vap}$ is the isotopic signature of the water vapour of the chamber
 231 atmosphere and ε_{atm}^* is the equilibrium fractionation inside the chamber at the specific
 232 sampling date. The signature of the atmospheric water vapour was measured on its
 233 condensate ($\delta^{18}\text{O}_{atm,cond}$) collected in the peltier water trap, which was therefore
 234 corrected with the equilibrium fractionation during condensation inside the peltier-
 235 cooled water condenser (ε_{pelt}^*).

236 The kinetic fractionation due to the difference in molecular diffusivity of the water
 237 molecule species ($\varepsilon^k = 20.7 \text{ ‰ } \delta^{18}\text{O}$ and $10.8 \text{ ‰ } \delta^2\text{H}$) was estimated according to
 238 Cappa et al. (2003) for a laminar boundary layer (Schmidt-number $q = 2/3$,
 239 Dongmann et al. 1974). The equilibrium fractionation due to the phase change during
 240 evaporation and condensation at different temperatures was calculated as in Majoube
 241 (1971) with the conditions present at the specific day. The condensation (dew point)
 242 temperature inside the peltier-cooled water condenser ($T_{pelt,DP}$) was determined based
 243 on the remaining humidity and the air pressure of the air leaving the condenser
 244 (details on the calculation are given in Appendix B). The equilibrium fractionation
 245 factors during the labelling experiment were on average $\varepsilon_{atm}^* = 8.9 \pm 0.2 \text{ ‰}$ for $\delta^{18}\text{O}$
 246 and $72.7 \pm 2.7 \text{ ‰}$ for $\delta^2\text{H}$ at $T = 31.3 \pm 2.7 \text{ °C}$ inside the labelling chamber and $\varepsilon_{pelt}^* =$
 247 $11.1 \pm 0.2 \text{ ‰}$ for $\delta^{18}\text{O}$ and $103.3 \pm 3.3 \text{ ‰}$ for $\delta^2\text{H}$ at $T_{pelt,DP} = 6.0 \pm 2.5 \text{ °C}$ inside the
 248 water condenser.

249 We compared the distribution of the assimilated labels (^{13}C , ^{18}O , ^2H) in the leaf, stem
 250 and root tissue by its isotopic ratios. Therefore we converted the δ -notation to atom
 251 fraction (Eqn 5) according to Coplen (2011).

$$252 \quad x(^{13}\text{C})_{t=x} = \frac{1}{1 + \frac{1}{(\delta^{13}\text{C}_{t=x}/1000 + 1) \cdot R_{V-PDB}}} \quad \text{Eqn 5}$$

253 , where $\delta^{13}\text{C}_{t=x}$ is the isotopic signature (in ‰) of the bulk tissue at sampling date x
 254 and R is the ratio of the heavier to the lighter isotope ($^{13}\text{C}/^{12}\text{C}$) of the international

255 standard V-PDB. The atom fraction of ^{18}O and ^2H was calculated accordingly, but
 256 using $R_{V\text{-SMOW}}$ as reference and neglecting the ^{17}O isotope amount.

257 For the Van Krevelen approach we calculated the elemental ratios. The relative
 258 label distribution ($^{18}\text{O}/^{13}\text{C}$ and $^2\text{H}/^{13}\text{C}$) within the plant organic matter (OM) was
 259 calculated based on the excess atom fraction measured in each tissue (Eqn 6).

$$260 \quad \frac{x^E(^{18}\text{O}_{\text{tissue, OM}})_{t=x/t=0}}{x^E(^{13}\text{C}_{\text{tissue, OM}})_{t=x/t=0}} = \frac{x(^{18}\text{O}_{\text{tissue, OM}})_{t=x} - x(^{18}\text{O}_{\text{tissue, OM}})_{t=0}}{x(^{13}\text{C}_{\text{tissue, OM}})_{t=x} - x(^{13}\text{C}_{\text{tissue, OM}})_{t=0}} \quad \text{Eqn 6}$$

261 , where $x^E(^{18}\text{O})_{t=x/t=0}$ and $x^E(^{13}\text{C})_{t=x/t=0}$ is the excess atom fraction of the labels detected
 262 at a specific sampling date ($t = x$), relative to the unlabelled control ($t = 0$). Eqn 6 and
 263 7 was analogously calculated for the $^2\text{H}/^{13}\text{C}$ ratio.

264 In a second step we corrected the isotopic ratios ($^{18}\text{O}/^{13}\text{C}$ and $^2\text{H}/^{13}\text{C}$) with the
 265 maximum label strength (Eqn 7), which was assumed to be the excess atom fraction
 266 of ^{13}C in the leaf water-soluble organic matter (wsOM) and the excess atom fraction
 267 of ^{18}O and ^2H in the leaf water (relative to the unlabelled control).

$$268 \quad \frac{x^E_{\text{norm}}(^{18}\text{O}_{\text{tissue, OM}})_{t=x/t=0}}{x^E_{\text{norm}}(^{13}\text{C}_{\text{tissue, OM}})_{t=x/t=0}} = \frac{x^E(^{18}\text{O}_{\text{tissue, OM}})_{t=x/t=0}}{x^E(^{13}\text{C}_{\text{tissue, OM}})_{t=x/t=0}} \cdot \frac{x^E(^{13}\text{C}_{\text{leaf, wsOM}})_{t=x/t=0}}{x^E(^{18}\text{O}_{\text{leaf, water}})_{t=x/t=0}} \quad \text{Eqn 7}$$

269 **3 Results**

270 **3.1 Labelling of the leaf water and water-soluble OM**

271 The ^{18}O and ^2H label added as water vapour to the chamber atmosphere ($\delta^{18}\text{O} = -$ 370
 272 ‰ , $\delta^2\text{H} = -$ 813 ‰), was mixed with transpired water, which was isotopically
 273 enriched compared to the added label (Fig. 1). The isotopic signature of the water
 274 vapour within the chamber air stabilized after four days at a level of $- 112 \pm 4 \text{‰}$ $\delta^{18}\text{O}$
 275 and $- 355 \pm 7 \text{‰}$ $\delta^2\text{H}$. Thus the atmospheric water vapour signature was depleted in
 276 ^{18}O by $94 \pm 4 \text{‰}$ and in ^2H by $183 \pm 7 \text{‰}$ compared to the unlabelled atmosphere.

277 The leaf water was strongly depleted and its isotopic signature was stable at a level of
 278 $- 64 \pm 7 \text{‰}$ for $\delta^{18}\text{O}$ and $- 158 \pm 13 \text{‰}$ for $\delta^2\text{H}$ already after two days of labelling with
 279 the depleted water vapour (Fig. 1). The leaf water was thus on average depleted by 63
 280 $\pm 7 \text{‰}$ for $\delta^{18}\text{O}$ and $126 \pm 14 \text{‰}$ for $\delta^2\text{H}$ compared to the unlabelled leaf water
 281 signature and it was between the signature of the atmospheric water vapour and the
 282 water added to the soil ($\delta^{18}\text{O} = - 9 \pm 0 \text{‰}$, $\delta^2\text{H} = - 74 \pm 2 \text{‰}$). This indicates that a
 283 substantial amount of the leaf water originated from the atmospheric water pool,

284 suggesting that it entered the leaf via diffusion through the stomata. The depletion of
285 the water within a leaf was dependent on its position on the shoot (Fig. 2c,e). The leaf
286 water of the leaves sampled in the upper half of the shoot was $7 \pm 2 \text{ ‰}$ and $18 \pm 8 \text{ ‰}$
287 less depleted in $\delta^{18}\text{O}$ and $\delta^2\text{H}$ than the leaves sampled at the lower half. The isotopic
288 signature of the stem water ($\delta^{18}\text{O} = -10 \pm 0 \text{ ‰}$ and $\delta^2\text{H} = -74 \pm 4 \text{ ‰}$), as well as the
289 root ($\delta^{18}\text{O} = -6 \pm 1 \text{ ‰}$ and $\delta^2\text{H} = -58 \pm 4 \text{ ‰}$) and the soil water ($\delta^{18}\text{O} = -6 \pm 1 \text{ ‰}$
290 and $\delta^2\text{H} = -63 \pm 3 \text{ ‰}$), was not significantly depleted and reflected the signature of
291 the water added to the soil (Fig. 1).

292 At the second sampling date, the leaf water seemed to be more depleted than the water
293 vapour within the chamber air (Fig. 1). This is the result of different sampling
294 procedures. The leaf sampling was performed at one point in time (three hours after
295 the light switched on), while the atmospheric water vapour collected by condensation
296 represents an average on the previous 24 hours. Therefore the depletion of the water
297 vapour is underestimated before the equilibrium of the isotopic signature in the
298 atmosphere was reached. In the following the average values of signatures detected
299 after the equilibrium was reached are given ($t = 8$ and $t = 14$). We tried to estimate the
300 contribution of the isotopic signature of the atmospheric water vapour that enters the
301 leaf by diffusion with a two-source mixing model (Tab. 1). The results were obtained
302 by the two water isotopes ^{18}O and ^2H separately. Both indicated a substantial
303 contribution of the atmospheric water vapour to the leaf water isotopic signature,
304 whereby the estimates based on the oxygen isotope yielded a higher contribution (69
305 $\pm 7 \text{ ‰}$) than the hydrogen estimates ($58 \pm 4 \text{ ‰}$). The estimates for the leaves sampled
306 at different position on the shoot varied by 5 ‰ , whereas the contribution of
307 atmospheric water to the leaf water was higher in the leaves sampled at the bottom
308 ($71 \pm 4 \text{ ‰}$ based on ^{18}O and $60 \pm 2 \text{ ‰}$ based on ^2H) than in the leaves at the top ($66 \pm$
309 2 ‰ and $55 \pm 0 \text{ ‰}$, respectively) of the shoots.

310 The ^{13}C - CO_2 added ($8938 \text{ ‰ } \delta^{13}\text{C}$) was assumingly also strongly diluted by respired
311 ^{12}C - CO_2 , but we did not measure the isotopic signature of the CO_2 within the chamber
312 air. The leaf water-soluble OM was significantly enriched already after one day of
313 labelling and levelled off towards the end of the experiment. At the last two sampling
314 dates its isotopic signature was on average $1346 \pm 162 \text{ ‰ } \delta^{13}\text{C}$.

315 **3.2 Labelling of the bulk organic matter**

316 All three applied labels could be detected in the plant bulk material (Tab. 2). We
317 measured the isotopic signature of the non-exchangeable hydrogen, which was
318 estimated to be 74 ± 1 % of the total OM. After fourteen days of continuous labelling,
319 the leaves, petioles, stems and roots were enriched by 650 - 1150 ‰ in $\delta^{13}\text{C}$, depleted
320 by 4 - 17 ‰ in $\delta^{18}\text{O}$ and 6 - 31 ‰ in $\delta^2\text{H}$. Thus the plant biomass was significantly
321 labelled even under the extreme environmental conditions (high temperature and low
322 light availability) that were critical for net C assimilation (increasing tissue respiration
323 and reducing photosynthesis, respectively). However, the labelling was not strong
324 enough to trace the OM within the large OM pools of the cuttings and soil organic
325 matter, in which the change in isotopic signature was close to the detection limit or
326 could not be detected. The measured depletion in ^{18}O of the bulk soil can be
327 accounted for natural variability, since the same effect has been observed in non-
328 treated soil (data not shown here).

329 The labelling of the leaf bulk OM occurred in parallel to the labelling of the leaf water
330 and water-soluble OM (Fig. 2). The leaf OM was enriched in ^{13}C after one day (Fig.
331 2b) and depleted in ^{18}O and ^2H after two days (Fig. 2d,f). The incorporation of the
332 label into the leaf OM was, as the labelling of the leaf water, dependent on the
333 position on the shoot. The biomass of the leaves at the top was more enriched in ^{13}C
334 (by up to 673 ‰) than the biomass of the leaves at the bottom of the shoots, and in
335 contrast to the leaf water, more depleted in ^{18}O and ^2H (by up to 9 and 21 ‰,
336 respectively) at the top than at the bottom. This indicates a higher overall assimilation
337 in the leaves at the top of the shoot.

338 **3.3 Atomic and isotopic ratios to characterize organic matter**

339 The atomic ratios of the plant bulk OM were in the range of 13.7 - 115.4 C/N, 0.70 -
340 0.83 O/C and 1.56 - 1.72 H/C (Tab. 3). The leaf OM was characterized by the lowest
341 C/N and O/C ratios and concurrently by highest H/C ratios (Fig. 3a). The other plant
342 tissues indicated a linear trend in decreasing O/C and H/C and increasing C/N ratios
343 in the order of stems, petioles, roots and cuttings.

344 The recovery of the three isotopes varied between the leaf, stem and root tissue, while
345 they were similar between the sampling dates (Fig. 3b). The isotopic ratios of the
346 excess atom fractions were $3.5 \pm 0.4 \times 10^{-3} \text{ }^{18}\text{O}/^{13}\text{C}$ and $5.3 \pm 0.5 \times 10^{-4} \text{ }^2\text{H}/^{13}\text{C}$ in the
347 leaves, $1.4 \pm 0.1 \times 10^{-3} \text{ }^{18}\text{O}/^{13}\text{C}$ and $2.9 \pm 0.6 \times 10^{-4} \text{ }^2\text{H}/^{13}\text{C}$ in the stems and $1.0 \pm 0.2 \times$

348 $10^{-3} \text{ }^{18}\text{O}/^{13}\text{C}$ and $1.0 \pm 1.4 \times 10^{-4} \text{ }^2\text{H}/^{13}\text{C}$ in the roots after the equilibrium in the leaf
349 water and water-soluble OM labelling was reached. Thus the $^{18}\text{O}/^{13}\text{C}$ ratios were on
350 average 2.6 (± 0.2) times lower in the stems and 3.8 (± 0.7) times lower in the roots
351 than in the leaves (Tab. 3) and the $^2\text{H}/^{13}\text{C}$ ratios 1.9 (± 0.2) and 3.1 (± 0.6) times lower
352 in the stems and roots, respectively, than in the leaves.

353 After correction for the maximum label strength (^{18}O , ^2H and ^{13}C excess atom fraction
354 within the leaf water and the water-soluble OM, respectively), the isotopic ratios were
355 in the range of 0.17 - 0.43 $^{18}\text{O}/^{13}\text{C}$ and 0.14 - 0.23 $^2\text{H}/^{13}\text{C}$. The normalized isotopic
356 ratios were thus in the magnitude order of the atomic ratios reported for OM
357 compounds (Tab. 3, Fig. 3c), however lower than expected for fresh organic matter
358 (in the range characteristic for condensed hydrocarbons).

359 **4 Discussion**

360 **4.1 Diffusion of atmospheric water vapour into the leaf**

361 The strong depletion in $\delta^{18}\text{O}$ and $\delta^2\text{H}$ observed in the leaf water indicates a high back-
362 diffusion of labelled water vapour from the atmosphere into the leaf. The diffusion is
363 dependent on the gradient between atmospheric and leaf water vapour pressure and
364 the stomatal conductance (Parkhurst, 1994). The higher the atmospheric water vapour
365 pressure (the smaller the gradient), the more water molecules diffuse back into the
366 leaf. The latter is further enhanced the larger the stomatal conductance is (Reynolds
367 Henne, 2007). Here we maintained the atmospheric vapour pressure constant at a high
368 level, ensuring a high back-diffusion at a given stomatal conductance. In our
369 experiment the leaf water $\delta^{18}\text{O}$ and $\delta^2\text{H}$ signature is determined by i) the signature and
370 the amount of labelled (depleted) water vapour diffusing into the leaf intercellular
371 cavities, ii) by the enrichment due to transpiration (kinetic and equilibrium
372 fractionation) and iii) by the influx of xylem water, which is isotopically enriched
373 relative to the labelled water vapour. The latter is proportionally enhanced by
374 increasing transpiration rates as a result of the diffusion convection process of H_2O
375 (Péclet effect, Farquhar and Lloyd 1993).

376 The distinct label signal in the water sampled in leaves at different positions on the
377 shoot indicates differences in the transpiration rate. Meinzer et al. (1997)
378 demonstrated in large poplar trees that shading or lower irradiance leads to lower
379 stomatal conductance and transpiration rates. Thus the back-diffusion in the leaves on

380 the bottom might have been reduced due to lower stomatal conductance. However, the
381 increased transpiration in the leaves at the top, lead to an even stronger dilution of the
382 isotopic signal in the leaf water due to i) increased evaporative leaf water enrichment
383 and ii) the Péclet effect (enhanced influx of xylem water, which was enriched
384 compared to the labelled atmospheric water vapour).

385 The amount of leaf water that entered the leaf by back-diffusion was estimated to be
386 58-69 %. This result is in contradiction to the common perception that most of the leaf
387 water is taken up from the soil via roots. However it is in line with the observations
388 made by Farquhar & Cernusak (2005), who modelled the leaf water isotopic
389 composition in the non-steady state and estimated the contribution of atmospheric
390 water to the leaf water to be approximately two-thirds of the total water supply.
391 Albeit, our estimates are based on a modelling approach that does not take into
392 account the Péclet effect or daily fluctuations in the isotopic signatures as described
393 below, our estimates correspond very well the findings of Farquhar & Cernusak
394 (2005).

395 The model used to estimate the quantitative contribution of the two water sources is
396 based on the measured signature of the leaf water ($\delta^{18}\text{O}_{\text{leaf,water}}$) and the estimated
397 signatures of the water at the evaporating and condensation site ($\delta^{18}\text{O}_{\text{source,1}}$ and
398 $\delta^{18}\text{O}_{\text{source,2}}$, respectively). The “dilution” of the (laminar) leaf water with the relatively
399 enriched xylem water through the Péclet effect is included in the $\delta^{18}\text{O}_{\text{leaf,water}}$. This
400 explains the lower contribution of atmospheric water (- 5 %) estimated in the leaves
401 sampled at the top (due to the Péclet effect resulting from higher transpiration rates)
402 compared to the leaves sampled at the bottom of the shoot.

403 Some inaccuracy in the two-source mixing model estimates might have been
404 introduced by daily fluctuations in the environmental and labelling conditions. The
405 mixture ($\delta^{18}\text{O}_{\text{leaf,water}}$) was sampled after three hours of light, whereas the estimation
406 of the two sources ($\delta^{18}\text{O}_{\text{source,1}}$ and $\delta^{18}\text{O}_{\text{source,2}}$) is based on daily average values of
407 environmental parameters and the atmospheric water vapour ($\delta^{18}\text{O}_{\text{atm.vap}}$) label
408 strength. In our experiment, fluctuations in $\delta^{18}\text{O}_{\text{atm.vap}}$ were caused by adding the
409 labelled vapour mainly during night-time, when transpiration was low. Thus the
410 atmospheric label strength was assumingly highest before the lights were switched on
411 and gradually diluted during the day by transpired water vapour. Hence the actual
412 $\delta^{18}\text{O}_{\text{atm.vap}}$ at the time of plant sampling was probably more depleted than the

413 measured average signature. Therefore $\delta^{18}\text{O}_{\text{source},2}$ and its contribution to the leaf
414 water was slightly overestimated. The effect of the temperature fluctuations ($\pm 3\text{ }^\circ\text{C}$)
415 via changes in the equilibrium fractionation was minor for the outcome of the mixing
416 model $< 1\%$.

417 Nonetheless, the strong depletion of the leaf water in ^2H and ^{18}O proofs, that back-
418 diffusion of atmospheric water vapour into the leaf is an important mechanisms for
419 leaf water uptake. Atmospheric water vapour diffusion might be as important as the
420 flux of water from the xylem into the leaf (at least under humid conditions) and be an
421 important mechanisms for the reversed water flow observed in the tropics (Goldsmith,
422 2013).

423 **4.2 Tracing organic matter?**

424 The O/C and H/C ratio of the plant bulk material was close to the signature of
425 cellulose (Fig. 3a). The leaves had a lower O/C ratio with a constant high H/C ratio
426 indicating that its OM contains more reduced compounds such as amino-sugars or
427 proteins, which is also supported by its low C/N ratio. The trend of decreasing O/C
428 and H/C ratios observed in the other tissues is in the direction of condensation
429 reactions. This trend most likely indicates the increasing lignification of OM from
430 shoots, to roots, to cuttings.

431 The same trend has been observed in the ratios of the labels added from the leaf, to
432 the stem, to the root OM (Fig. 3b,c). The lower isotopic O/C and H/C ratios in the
433 root and stem tissue compared to the leaf tissue could indicate the utilization of the
434 labelled assimilates for the synthesis of more condensed compounds (e.g. lignin) in
435 those tissues. However, other factors affecting the isotopic ratios of the OM are the
436 maximum label strength, the exchange of hydrogen and oxygen with xylem water
437 during transport and biosynthesis and the isotopic fractionation during metabolism.

438 The isotopic ratios (Fig. 3b) were around three magnitudes smaller than the expected
439 atomic ratios of OM (Sleighter and Hatcher, 2007). This is mainly due to the different
440 maximum label strength, which was highest for the ^{13}C and lowest for the ^2H . After
441 correction for this factor, the isotopic ratios were in the range of the atomic ratios
442 characteristic for condensed hydrocarbons (Fig. 3c). The isotopic ratios might be
443 lower than expected due to inaccurate approximation of the maximum label strength
444 of fresh assimilates (by the leaf water and water-soluble OM), or be the result of ^{18}O
445 and ^2H label losses during transport and biosynthesis.

446 One reason for the label loss might be the use of other (more enriched) sources during
447 biosynthesis. For example O₂ (enriched by 23 ‰ δ¹⁸O) has been identified as a further
448 source for aromatic compounds, such as phenols and sterols (Schmidt et al., 2001).
449 However, for hydrogen, water is the only known source (Schmidt et al., 2003) and
450 therefore the use of other O or H sources during biosynthesis can not explain the
451 (major) loss of the ¹⁸O and ²H label.

452 Another potential reason would be the kinetic fractionation during biosynthesis that
453 leads to distinct isotopic signatures of different OM compounds (described in Schmidt
454 et al. 2001, 2003; Badeck et al. 2005; Bowling et al. 2008). However, assuming
455 constant isotopic fractionation during the experimental period (constant
456 environmental conditions), the isotopic ratios would not be affected, since they are
457 based on the excess atom fraction relative to the unlabelled OM.

458 A third reason for the loss of the ¹⁸O and ²H label could be the exchange of hydrogen
459 and oxygen atoms with water. O and H exchanges with tissue water during transport
460 and the synthesis of new compounds (as recently discussed for oxygen in phloem
461 sugars and cellulose in Offermann et al. 2011 and Gessler et al. 2013). O of carbonyl
462 groups (Barbour, 2007; Sternberg et al., 1986) and H in nucleophilic OH and NH
463 groups or H adjacent to carbonyl groups (Augusti et al., 2006; Garcia-Martin et al.,
464 2001) exchange with water. Thus biochemical reactions lead to different isotopomers
465 of organic compounds (Augusti and Schleucher, 2007). The proportion of O and H
466 exchanged can be considerable, e.g. during cellulose synthesis around 40 % of O and
467 H are exchanged with the tissue water (Roden and Ehleringer, 1999; Yakir and
468 DeNiro, 1990). The exchange with water explains to some extent the stronger relative
469 ¹⁸O and ²H signal in the leaf OM compared to the stem and root OM, since the leaf
470 water was labelled, while the stem and root water was not. Especially the ¹⁸O/¹³C
471 isotopic ratios were increased in the leaf OM compared to the relations observed in
472 the atomic ratios (Fig. 3a). The leaf OM has the lowest O/C atomic ratios while it has
473 the highest ¹⁸O/¹³C isotopic ratios of all plant compartments (Tab. 3). This effect is
474 less expressed for the ²H/¹³C ratios, since only the fraction of hydrogen that does not
475 exchange with ambient water vapour is measured. The non-exchangeable fraction (74
476 %) is hydrogen bound to carbon (Filot et al., 2006), which is hardly exchanged with
477 xylem water.

478 **5 Conclusions**

479 We present a new technique to label organic matter at its place of formation by the
480 application of labels through the gaseous phase ($^{13}\text{CO}_2$ and $^2\text{H}_2^{18}\text{O}$). In this study we
481 could show that in a humid atmosphere, the atmospheric water vapour isotopic
482 signature dominates the leaf water signature, due to a strong back-diffusion of water
483 vapour into the leaf. Further we detected differences in the relative distribution of ^{13}C ,
484 ^{18}O and ^2H in the leaves, stems and roots. This could indicate the synthesis of
485 different compounds in the particular tissues (change in OM characteristics), but it
486 could also be the result of exchange and fractionation processes during transport and
487 biosynthesis. To further test these two possibilities a better estimation of the
488 maximum label strength by compound specific sugar analysis would be needed,
489 which has been further developed for $\delta^{13}\text{C}$ (Rinne et al., 2012) and for $\delta^{18}\text{O}$ (Zech et
490 al., 2013) recently, but does not yet exist for $\delta^2\text{H}$ analysis.

491 The multi-isotope labelling technique can be used to assess the amount of vapour
492 diffusing into the leaves and to trace the dynamics of the labelled organic matter. It
493 could be applied in soil sciences, e.g. to track the decomposition pathways of soil OM
494 inputs, or in the field of plant physiology and paleoclimatic reconstruction, e.g. to
495 further investigate the O and H exchange and fractionation processes during transport
496 and metabolic processes or the importance of the ambient air humidity besides its
497 isotopic composition for the climate signal stored in tree-ring cellulose. Furthermore
498 the multi-isotope labelling technique has the potential to make changes of OM
499 characteristics visible (e.g. C allocation into the non-structural vs. structural pool), for
500 example after a change in climatic conditions, and to trace the labelled OM during its
501 decomposition within the soil.

502 **Acknowledgements**

503 This study was funded by the Swiss National Science Foundation (SNSF), project
504 number 135233. We would like to thank Professor M. W. I Schmidt for his support,
505 M. Saurer for his comments on the manuscript, R. Künzli, I. Lötscher, R. Maier, P.
506 Nyfeler and I. Woodhatch for technical assistance, and the soil science and
507 biogeochemistry (University of Zurich) and the ecosystem fluxes (Paul Scherrer
508 Institute) research groups for valuable discussions.

509 **References**

510 Augusti, A., Betson, T. R. and Schleucher, J.: Hydrogen exchange during cellulose
511 synthesis distinguishes climatic and biochemical isotope fractionations in tree rings,
512 *New Phytol.*, 172, 490–499, doi:10.1111/j.1469-8137.2006.01843.x, 2006.

513 Augusti, A. and Schleucher, J.: The ins and outs of stable isotopes in plants, *New*
514 *Phytol.*, 174, 473–475, doi:10.1111/j.1469-8137.2007.02075.x, 2007.

515 Badeck, F.-W., Tcherkez, G., Nogués, S., Piel, C. and Ghashghaie, J.: Post-
516 photosynthetic fractionation of stable carbon isotopes between plant organs - a
517 widespread phenomenon, *Rapid Commun. Mass Spectrom.*, 19, 1381–1391,
518 doi:10.1002/rcm.1912, 2005.

519 Barbour, M. M.: Stable oxygen isotope composition of plant tissue: a review, *Funct.*
520 *Plant Biol.*, 34, 83–94, doi:10.1071/FP06228, 2007.

521 Bird, J. A. and Torn, M. S.: Fine roots vs. needles: a comparison of ¹³C and ¹⁵N
522 dynamics in a ponderosa pine forest soil, *Biogeochemistry*, 79, 361–382,
523 doi:10.1007/s10533-005-5632-y, 2006.

524 Bowling, D. R., Pataki, D. E. and Randerson, J. T.: Carbon isotopes in terrestrial
525 ecosystem pools and CO₂ fluxes, *New Phytol.*, 178, 24–40, doi:10.1111/j.1469-
526 8137.2007.02342.x, 2008.

527 Cappa, C. D., Hendricks, M. B., Depaolo, D. J. and Cohen, R. C.: Isotopic
528 fractionation of water during evaporation, *J. Geophys. Res.*, 108, 4525,
529 doi:10.1029/2003JD003597, 2003.

530 Coplen, T. B.: Guidelines and recommended terms for expression of stable-isotope-
531 ratio and gas-ratio measurement results, *Rapid Commun. Mass Spectrom.*, 25,
532 2538–2560, doi:10.1002/rcm.5129, 2011.

533 Craig, H. and Gordon, L. I.: Deuterium and oxygen 18 variations in the ocean and the
534 marine atmosphere, in *Stable isotopes in oceanographic studies and*
535 *paleotemperatures*, edited by E. Tongiorgi, pp. 9–130, Spoleto, Pisa, Italy., 1965.

536 Dawson, T. E., Mambelli, S., Plamboeck, A. H., Templer, P. H. and Tu, K. P.: Stable
537 isotopes in plant ecology, *Annu. Rev. Ecol. Syst.*, 33, 507–559,
538 doi:10.1146/annurev.ecolsys.33.020602.095451, 2002.

539 Dongmann, G., Nürnberg, H. W., Förstel, H. and Wagener, K.: On the enrichment of
540 H₂¹⁸O in the leaves of transpiring plants, *Radiat. Environ. Biophys.*, 11, 41–52,
541 doi:10.1007/BF01323099, 1974.

542 Farquhar, G. D. and Cernusak, L. A.: On the isotopic composition of leaf water in the
543 non-steady state, *Funct. Plant Biol.*, 32, 293–303, doi:10.1071/FP04232, 2005.

544 Farquhar, G. D. and Lloyd, J.: Carbon and oxygen isotope effects in the exchange of
545 CO₂ between terrestrial plants and the atmosphere, in *Stable isotopes and plant*
546 *carbon-water relations*, edited by J. R. Ehleringer, A. E. Hall, and G. D. Farquhar,
547 pp. 47–70, Academic Press, Waltham., 1993.

548 Filot, M.: Isotopes in tree-rings: Development and application of a rapid preparative
549 online equilibration method for the determination of D / H ratios of
550 nonexchangeable hydrogen in tree-ring cellulose, 106 pp., Bern., 2010.

551 Filot, M. S., Leuenberger, M., Pazdur, A. and Boettger, T.: Rapid online equilibration
552 method to determine the D/H ratios of non-exchangeable hydrogen in cellulose,
553 *Rapid Commun. Mass Spectrom.*, 20, 3337–3344, doi:10.1002/rcm, 2006.

554 Garcia-Martin, M. L., Ballesteros, P. and Cerda, S.: The metabolism of water in cells
555 and tissues as detected by NMR methods, *Prog. Nucl. Magn. Reson. Spectrosc.*, 39,
556 41–77, doi:10.1016/S0079-6565(01)00031-0, 2001.

557 Gehre, M., Geilmann, H., Richter, J., Werner, R. A. and Brand, W. A.: Continuous
558 flow ²H/¹H and ¹⁸O/¹⁶O analysis of water samples with dual inlet precision, *Rapid*
559 *Commun. Mass Spectrom.*, 18, 2650–2660, doi:10.1002/rcm.1672, 2004.

560 Gessler, A., Brandes, E., Keitel, C., Boda, S., Kayler, Z. E., Granier, A., Barbour, M.,
561 Farquhar, G. D. and Treydte, K.: The oxygen isotope enrichment of leaf-exported
562 assimilates - does it always reflect lamina leaf water enrichment?, *New Phytol.*, 200,
563 144–157, doi:10.1111/nph.12359, 2013.

564 Girardin, C., Rasse, D. P., Biron, P., Ghashghaie, J. and Chenu, C.: A method for ¹³C-
565 labeling of metabolic carbohydrates within French bean leaves (*Phaseolus vulgaris*
566 L.) for decomposition studies in soils, *Rapid Commun. Mass Spectrom.*, 23, 1792–
567 1800, doi:10.1002/rcm, 2009.

568 Goldsmith, G. R.: Changing directions : the atmosphere-plant-soil continuum, *New*
569 *Phytol.*, 199, 4–6, 2013.

570 Hangartner, S., Kress, A., Saurer, M., Frank, D. and Leuenberger, M.: Methods to
571 merge overlapping tree-ring isotope series to generate multi-centennial
572 chronologies, *Chem. Geol.*, 294, 127–134, doi:10.1016/j.chemgeo.2011.11.032,
573 2012.

574 Högberg, P., Högberg, M. N., Göttlicher, S. G., Betson, N. R., Keel, S. G., Metcalfe,
575 D. B., Campbell, C., Schindlbacher, A., Hurry, V., Lundmark, T., Linder, S. and

576 Näsholm, T.: High temporal resolution tracing of photosynthate carbon from the tree
577 canopy to forest soil microorganisms, *New Phytol.*, 177, 220–228,
578 doi:10.1111/j.1469-8137.2007.02238.x, 2008.

579 Keel, S. G., Siegwolf, R. T. W. and Körner, C.: Canopy CO₂ enrichment permits
580 tracing the fate of recently assimilated carbon in a mature deciduous forest, *New*
581 *Phytol.*, 172, 319–329, doi:10.1111/j.1469-8137.2006.01831.x, 2006.

582 Kim, S., Kramer, R. W. and Hatcher, P. G.: Graphical method for analysis of
583 ultrahigh-resolution broadband mass spectra of natural organic matter, the van
584 Krevelen diagram, *Anal. Chem.*, 75, 5336–5344, doi:10.1021/ac034415p, 2003.

585 Kulmatiski, A., Beard, K. H., Verweij, R. J. T. and February, E. C.: A depth-
586 controlled tracer technique measures vertical, horizontal and temporal patterns of
587 water use by trees and grasses in a subtropical savanna, *New Phytol.*, 188, 199–209,
588 doi:10.1111/j.1469-8137.2010.03338.x, 2010.

589 Majoube, M.: Fractionnement en oxygène 18 et en deutérium entre l'eau et sa vapeur,
590 *J. Chim. Phys. physico-chimie Biol.*, 68, 1423–1435, 1971.

591 Meinzer, F. C., Hinckley, T. M. and Ceulemans, R.: Apparent responses of stomata to
592 transpiration and humidity in a hybrid poplar canopy, *Plant, Cell Environ.*, 20,
593 1301–1308, doi:10.1046/j.1365-3040.1997.d01-18.x, 1997.

594 Offermann, C., Ferrio, J. P., Holst, J., Grote, R., Siegwolf, R. T. W., Kayler, Z. E. and
595 Gessler, A.: The long way down-are carbon and oxygen isotope signals in the tree
596 ring uncoupled from canopy physiological processes?, *Tree Physiol.*, 31, 1088–
597 1102, doi:10.1093/treephys/tpr093, 2011.

598 Ohno, T., He, Z., Sleighter, R. L., Honeycutt, C. W. and Hatcher, P. G.: Ultrahigh
599 resolution mass spectrometry and indicator species analysis to identify marker
600 components of soil- and plant biomass- derived organic matter fractions, *Environ.*
601 *Sci. Technol.*, 44, 8594–8600, doi:10.1021/es101089t, 2010.

602 Parkhurst, D. F.: Tansley review no. 65. Diffusion of CO₂ and other gases inside
603 leaves, *New Phytol.*, 126, 449–479, doi:10.1111/j.1469-8137.1994.tb04244.x, 1994.

604 Plamboeck, A. H., Dawson, T. E., Egerton-Warburton, L. M., North, M., Bruns, T. D.
605 and Querejeta, J. I.: Water transfer via ectomycorrhizal fungal hyphae to conifer
606 seedlings, *Mycorrhiza*, 17, 439–447, doi:10.1007/s00572-007-0119-4, 2007.

607 Reynolds Henne, C. E.: A study of leaf water $\delta^{18}\text{O}$ composition using isotopically-
608 depleted H₂¹⁸O-vapour, in *Climate-isotope relationships in trees under non-limiting*

609 climatic conditions from seasonal to century scales, pp. 77–92, University of Bern.,
610 2007.

611 Rinne, K. T., Saurer, M., Streit, K. and Siegwolf, R. T. W.: Evaluation of a liquid
612 chromatography method for compound-specific $\delta^{13}\text{C}$ analysis of plant carbohydrates
613 in alkaline media, *Rapid Commun. Mass Spectrom.*, 26, 2173–85,
614 doi:10.1002/rcm.6334, 2012.

615 Roden, J. S. and Ehleringer, J. R.: Hydrogen and oxygen isotope ratios of tree-ring
616 cellulose for riparian trees grown long-term under hydroponically controlled
617 environments, *Oecologia*, 121, 467–477, doi:10.1007/s004420050953, 1999.

618 Roden, J. S. and Farquhar, G. D.: A controlled test of the dual-isotope approach for
619 the interpretation of stable carbon and oxygen isotope ratio variation in tree rings,
620 *Tree Physiol.*, 32, 1–14, doi:10.1093/treephys/tps019, 2012.

621 Scheidegger, Y., Saurer, M., Bahn, M. and Siegwolf, R. T. W.: Linking stable oxygen
622 and carbon isotopes with stomatal conductance and photosynthetic capacity: A
623 conceptual model, *Oecologia*, 125, 350–357, doi:10.1007/S004420000466, 2000.

624 Schenck zu Schweinsberg-Mickan, M., Joergensen, R. G. and Müller, T.: Fate of ^{13}C -
625 and ^{15}N -labelled rhizodeposition of *Lolium perenne* as function of the distance to the
626 root surface, *Soil Biol. Biochem.*, 42, 910–918, doi:10.1016/j.soilbio.2010.02.007,
627 2010.

628 Schmidt, H.-L., Werner, R. A. and Eisenreich, W.: Systematics of ^2H patterns in
629 natural compounds and its importance for the elucidation of biosynthetic pathways,
630 *Phytochem. Rev.*, 2, 61–85, doi:10.1023/B:PHYT.0000004185.92648.ae, 2003.

631 Schmidt, H.-L., Werner, R. A. and Rossmann, A.: O-18 pattern and biosynthesis of
632 natural plant products, *Phytochemistry*, 58, 9–32, doi:10.1016/S0031-
633 9422(01)00017-6, 2001.

634 Simard, S. W., Durall, D. M. and Jones, M. D.: Carbon allocation and carbon transfer
635 between *Betula papyrifera* and *Pseudotsuga menziesii* seedlings using a ^{13}C pulse-
636 labeling method, *Plant Soil*, 191, 41–55, doi:10.1023/A:1004205727882, 1997.

637 Sleighter, R. L. and Hatcher, P. G.: The application of electrospray ionization coupled
638 to ultrahigh resolution mass spectrometry for the molecular characterization of
639 natural organic matter, *J. Massspectrometry*, 42, 559–574, doi:10.1002/jms, 2007.

640 Steinmann, K., Siegwolf, R. T. W., Saurer, M. and Körner, C.: Carbon fluxes to the
641 soil in a mature temperate forest assessed by ^{13}C isotope tracing, *Oecologia*, 141,
642 489–501, doi:10.1007/s00442-004-, 2004.

643 Sternberg, L. D. S. L. O., DeNiro, M. J. D. and Savidge, R. A.: Oxygen isotope
644 exchange between metabolites and water during biochemical reactions leading to
645 cellulose synthesis, *Plant Physiol.*, 82, 423–427, doi:10.1104/pp.82.2.423, 1986.

646 Studer, M. S., Siegwolf, R. T. W. and Abiven, S.: Carbon transfer, partitioning and
647 residence time in the plant-soil system: a comparison of two ¹³CO₂ labelling
648 techniques, *Biogeosciences*, 11, 1637–1648, doi:10.5194/bg-11-1637-2014, 2014.

649 Werner, C., Schnyder, H., Cuntz, M., Keitel, C., Zeeman, M. J., Dawson, T. E.,
650 Badeck, F.-W., Brugnoli, E., Ghashghaie, J., Grams, T. E. E., Kayler, Z. E., Lakatos,
651 M., Lee, X., Máguas, C., Ogée, J., Rascher, K. G., Siegwolf, R. T. W., Unger, S.,
652 Welker, J., Wingate, L. and Gessler, A.: Progress and challenges in using stable
653 isotopes to trace plant carbon and water relations across scales, *Biogeosciences*, 9,
654 3083–3111, doi:10.5194/bg-9-3083-2012, 2012.

655 Yakir, D. and DeNiro, M. J. D.: Oxygen and hydrogen isotope fractionation during
656 cellulose metabolism in *Lemna gibba* L., *Plant Physiol.*, 93, 325–332,
657 doi:10.1104/pp.93.1.325, 1990.

658 Zech, M., Saurer, M., Tuthorn, M., Rinne, K., Werner, R. a, Siegwolf, R., Glaser, B.
659 and Juchelka, D.: A novel methodological approach for $\delta(18)\text{O}$ analysis of sugars
660 using gas chromatography-pyrolysis-isotope ratio mass spectrometry., *Isotopes*
661 *Environ. Health Stud.*, 49, 492–502, doi:10.1080/10256016.2013.824875, 2013.

662

662 **Tables**

663 **Table 1.** Diffusion of atmospheric water vapour into the leaf water. $\delta^{18}\text{O}$ and $\delta^2\text{H}$
 664 signatures of leaf water and its two sources: i) the evaporating source (Eqn 3),
 665 estimated by the stem water signature plus kinetic and equilibrium leaf water
 666 enrichment (assuming full evaporation without back-diffusion), and ii) the
 667 condensation source (Eqn 4), assessed by the atmospheric water vapour signature plus
 668 equilibrium fractionation to account for the gas-liquid phase change. The contribution
 669 of the second source (diffusion and condensation of atmospheric water vapour) to the
 670 leaf water ($f_{\text{source},2/\text{leaf},\text{water}}$) was estimated by a two-source isotope mixing model for
 671 ^{18}O and ^2H separately (Eqn 2). Presented are the average values of three plant
 672 replicates for each sampling date \pm one standard deviation

Sampling date (days)	Leaf water ⁽¹⁾		Source 1: Evaporating source ⁽²⁾		Source 2: Condensation source ⁽²⁾		$f_{\text{source},2/\text{leaf},\text{water}}$ ⁽²⁾	
	$\delta^{18}\text{O}$ (‰)	$\delta^2\text{H}$ (‰)	$\delta^{18}\text{O}$ (‰)	$\delta^2\text{H}$ (‰)	$\delta^{18}\text{O}$ (‰)	$\delta^2\text{H}$ (‰)	^{18}O (%)	^2H (%)
0	-1.0 (± 0.5)	-32.0 (± 1.8)	21.3 (± 0.4)	10.9 (± 2.6)	-8.8	-99.7	74.2 (± 1.2)	38.8 (± 0.3)
1	-11.7 (± 1.8)	-53.0 (± 5.9)	19.5 (± 0.3)	10.3 (± 3.2)	-27.3	-143.3	66.6 (± 3.9)	41.2 (± 3.2)
2	-65.6 (± 6.5)	-162.3 (± 8.6)	20.0 (± 0.6)	14.4 (± 2.1)	-47.6	-196.0	126.6 (± 9.8)	84.0 (± 4.1)
8	-65.2 (± 2.0)	-159.9 (± 3.8)	20.0 (± 0.7)	5.3 (± 3.9)	-98.6	-274.8	71.8 (± 1.5)	59.0 (± 0.8)
14	-60.4 (± 10.7)	-152.3 (± 21.2)	19.3 (± 0.4)	9.5 (± 5.1)	-101.8	-275.8	65.8 (± 8.7)	56.8 (± 6.8)

⁽¹⁾ directly measured
⁽²⁾ calculated

673

673 **Table 2.** Multi-isotope labelling of bulk organic matter. $\delta^{13}\text{C}$, $\delta^{18}\text{O}$ and $\delta^2\text{H}$ signatures
674 (in ‰) of the plant-soil compartments (three replicates \pm one standard deviation)
675 measured before and after 1, 2, 8 and 14 days of continuous labelling. A significant
676 enrichment ($\delta^{13}\text{C}$) and depletion ($\delta^{18}\text{O}$, $\delta^2\text{H}$) compared to the unlabelled control (t =
677 0) is highlighted with * (t-test, P < 0.05). The degree of labelling is indicated by the
678 change in the isotopic signature of the last sampling date (t = 14) compared to the
679 control

		Sampling date (days)					
$\delta^{13}\text{C}$ (‰)	0	1	2	8	14	14 - 0 ⁽¹⁾	
Leaves	-30.8 (± 0.4)	161.5* (± 37.4)	189.7 (± 128.7)	570.7* (± 81.0)	812.5* (± 235.0)	843.3 ± 235.0	
Petioles	-32.8 (± 0.2)	163.9* (± 56.2)	212.8* (± 75.2)	908.5* (± 277.3)	941.9* (± 292.7)	974.7 ± 292.7	
Stems	-31.4 (± 0.6)	209.6* (± 84.2)	281.3* (± 87.6)	1093.7* (± 402.2)	1119.9* (± 367.6)	1151.3 ± 367.6	
Cuttings	-31.2 (± 0.3)	-27.0* (± 1.6)	-26.9 (± 1.9)	-14.6 (± 15.8)	-14.5* (± 2.1)	16.8 ± 2.1	
Roots	-30.8 (± 0.7)	98.1* (± 12.5)	90.8 (± 62.9)	646.5 (± 335.1)	618.0* (± 310.9)	648.8 ± 310.9	
Bulk soil	-28.0 (± 0.1)	-27.9 (± 0.0)	-27.8 (± 0.2)	-27.5 (± 0.5)	-27.5 (± 0.2)	0.5 ± 0.3	
$\delta^{18}\text{O}$ (‰)	0	1	2	8	14	14 - 0 ⁽¹⁾	
Leaves	25.9 (± 0.8)	25.2 (± 0.8)	21.9 (± 2.0)	15.0* (± 0.4)	9.0* (± 3.0)	-16.9 ± 3.2	
Petioles	21.0 (± 0.2)	20.4 (± 0.4)	19.5* (± 0.4)	14.3* (± 1.6)	12.8* (± 2.3)	-8.2 ± 2.3	
Stems	22.4 (± 0.4)	22.2 (± 0.1)	20.6* (± 0.8)	14.7* (± 2.4)	13.3* (± 2.8)	-9.1 ± 2.8	
Cuttings	21.3 (± 1.5)	21.9 (± 0.1)	21.8 (± 0.4)	21.5 (± 0.3)	21.5 (± 0.4)	0.2 ± 1.5	
Roots	21.2 (± 0.6)	20.6 (± 0.6)	20.9 (± 0.4)	18.2 (± 1.5)	17.5* (± 1.7)	-3.7 ± 1.8	
Bulk soil	14.8 (± 0.4)	14.0 (± 0.3)	13.8* (± 0.4)	13.0* (± 0.1)	13.5 (± 0.8)	-1.3 ± 0.9	
$\delta^2\text{H}$ (‰)	0	1	2	8	14	14 - 0 ⁽¹⁾	
Leaves	-146.6 (± 2.5)		-158.1 (± 7.8)	-169.2* (± 5.5)	-178.0* (± 9.4)	-31.3 ± 9.7	
Petioles	-138.3 (± 1.8)				-150.9 (± 6.7)	-12.6 ± 7.3	
Stems	-129.2 (± 4.2)		-136.3 (± 4.7)	-153.3 (± 14.8)	-152.9* (± 9.4)	-23.7 ± 10.3	
Cuttings	-167.3 (± 2.8)				-172.8 (± 6.3)	-5.5 ± 6.9	
Roots	-129.7 (± 6.4)		-134.0 (± 12.5)	-137.0 (± 6.8)	-135.9 (± 7.7)	-6.2 ± 10.0	
Bulk soil	-101.5 (± 1.1)				-101.9 (± 1.3)	0.4 ± 1.7	

⁽¹⁾ Isotopic difference for the entire labelling experiment

680 **Table 3.** Atomic and isotopic ratios of the labelled bulk organic matter. C/N, O/C and
 681 H/C atomic ratios and $^{18}\text{O}/^{13}\text{C}$ and $^2\text{H}/^{13}\text{C}$ isotopic ratios (of the excess atom fraction)
 682 measured in different plant compartments after the equilibrium in the atmospheric
 683 labelling was reached. Indicated are average values of two sampling dates (t = 8 and
 684 14) with three plant replicates each (\pm one standard deviation)

Compartment	C/N	O/C	H/C	$^{18}\text{O}/^{13}\text{C}^{(1)}$	$^2\text{H}/^{13}\text{C}^{(1)}$
Leaves	13.7 (± 0.4)	0.70 (± 0.01)	1.72 (± 0.04)	0.43 (± 0.07)	0.41 (± 0.06)
Petioles	35.4 (± 1.3)	0.77 (± 0.01)	1.64 (± 0.01)	0.18 (± 0.03)	0.14 (± 0.03) ⁽²⁾
Stems	32.0 (± 4.0)	0.83 (± 0.01)	1.71 (± 0.02)	0.17 (± 0.03)	0.23 (± 0.06)
Cuttings	115.4 (± 7.2)	0.72 (± 0.01)	1.56 (± 0.02)	n.m. ⁽³⁾	n.m. ⁽³⁾
Roots	29.9 (± 2.0)	0.73 (± 0.02)	1.61 (± 0.02)	0.12 (± 0.03)	0.07 (± 0.11)

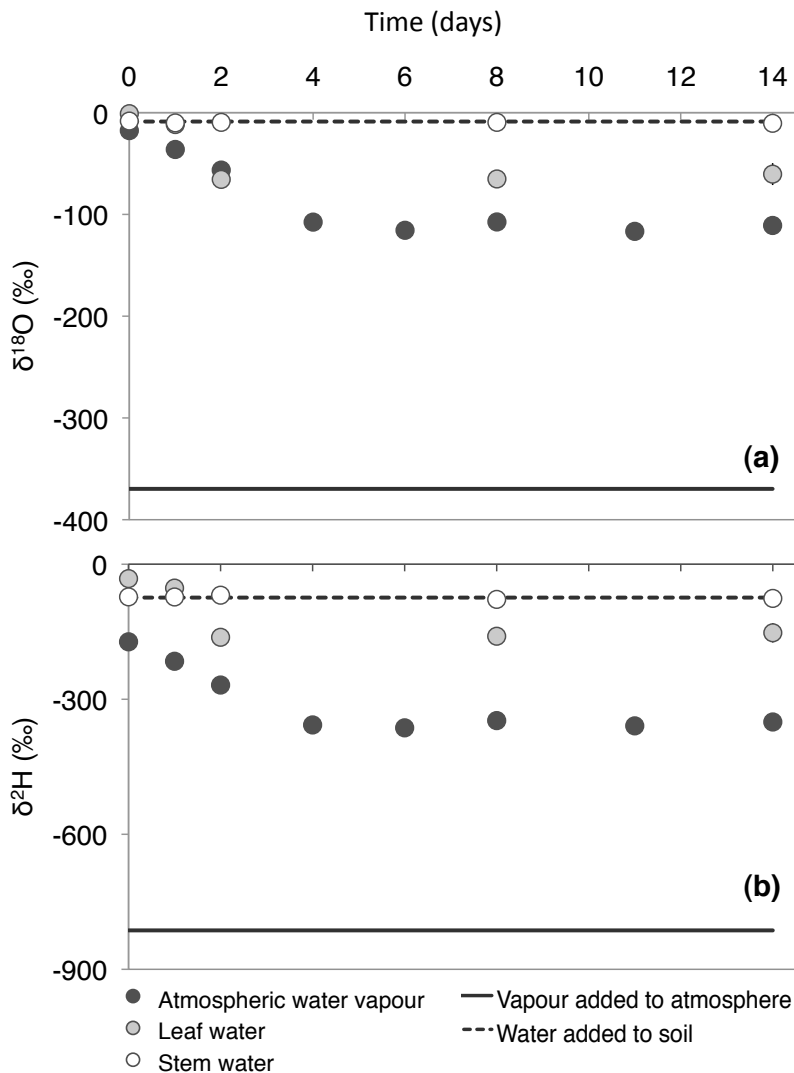
⁽¹⁾ Ratio of excess atom fraction normalized by the maximum label strength (Eqn 7)

⁽²⁾ Only the last sampling date was measured (t = 14)

⁽³⁾ Not measured

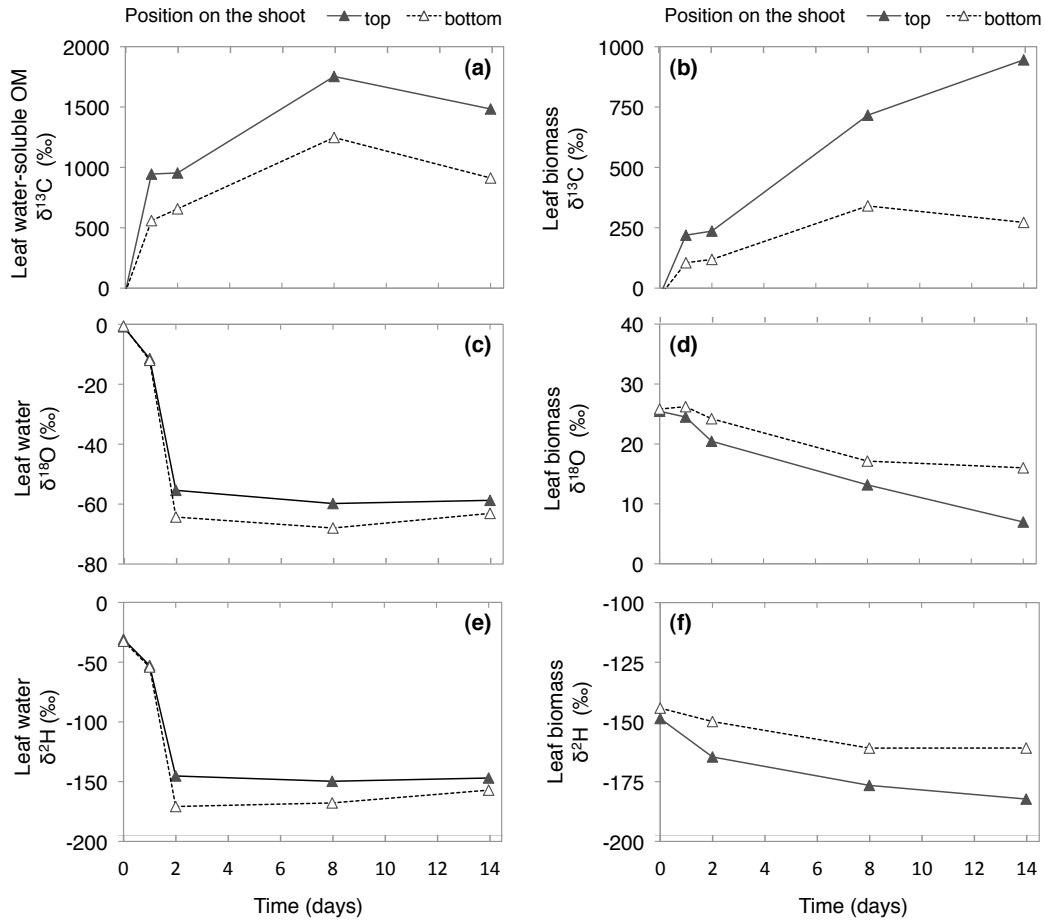
685

685 **Figures**

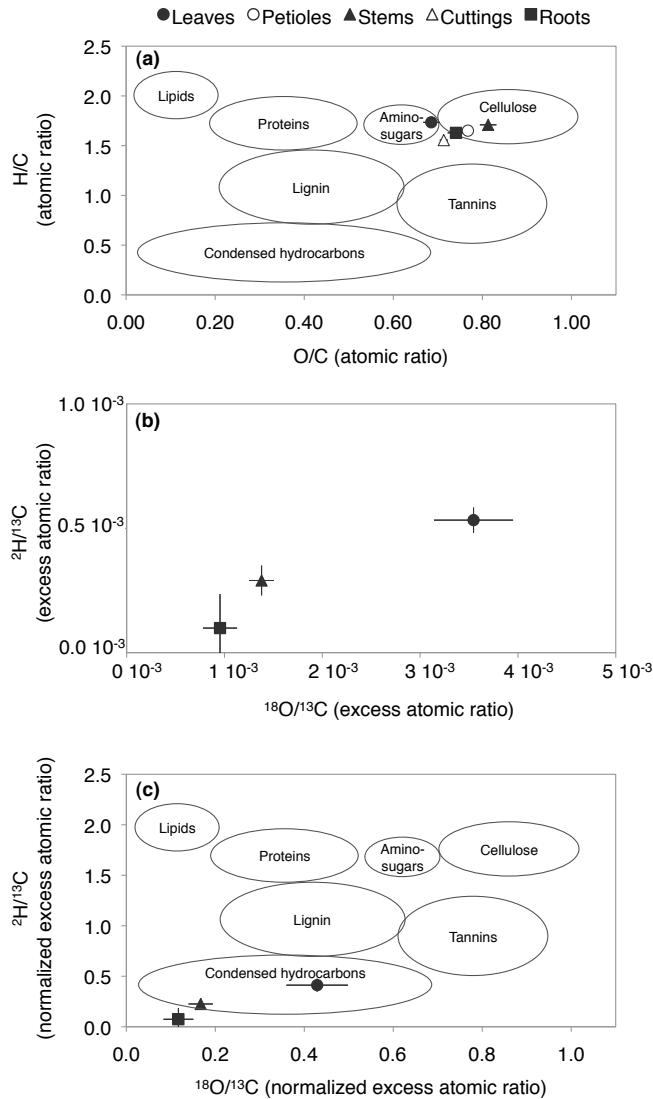


686

687 **Figure 1.** Temporal dynamics in the water isotopic signatures of the plant-soil-
 688 atmosphere system during continuous $^2\text{H}_2^{18}\text{O}$ labelling (a) $\delta^{18}\text{O}$ and (b) $\delta^2\text{H}$ signature
 689 (in ‰) of the depleted water label added as water vapour to the atmosphere (solid
 690 line), of the water added to the soil (dashed line), of the resulting water vapour in the
 691 chamber atmosphere (black dots) and of the extracted leaf water (white dots). Error
 692 bars on the leaf water indicate \pm one standard deviation of three plant replicates

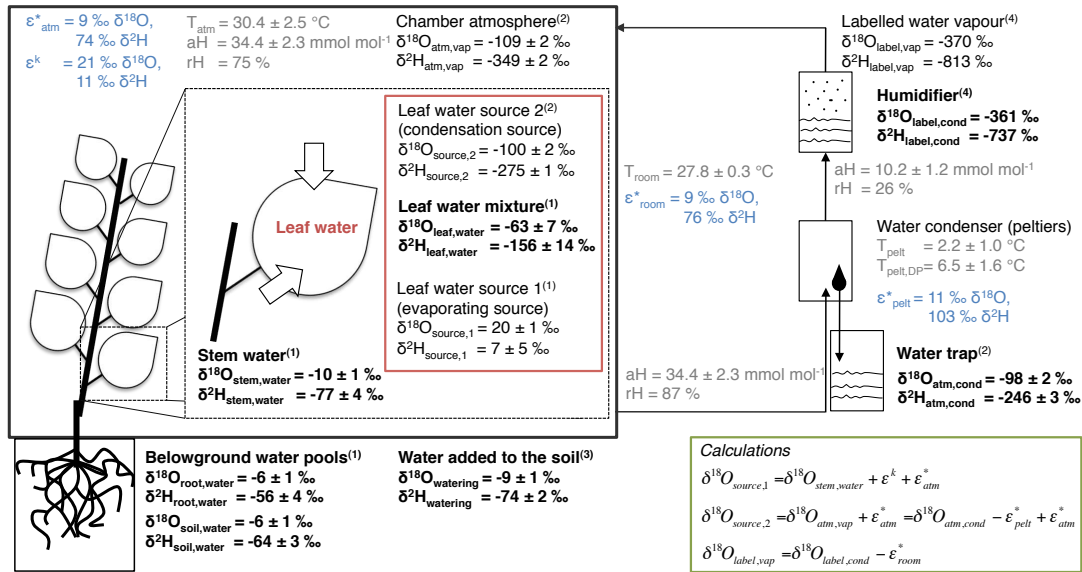


693
 694 **Figure 2.** Incorporation of the gaseous labels ($^{13}\text{CO}_2$, $^2\text{H}_2^{18}\text{O}$) into the leaf water
 695 water-soluble and bulk organic matter. (a,b) $\delta^{13}\text{C}$, (c,d) $\delta^{18}\text{O}$ and (e,f) $\delta^2\text{H}$ signature
 696 (in ‰) within leaves sampled at the top (solid line, black triangles), or at the bottom
 697 (dashed line, white triangles) of the shoot. Illustrated are the signatures of (a) the leaf
 698 water-soluble organic matter, (b,e,f) the leaf biomass and (c,e) the leaf water



699

700 **Figure 3.** Atomic and isotopic ratios to illustrate change in organic matter
 701 characteristics (a) Atomic and (b,c) isotopic ratios of oxygen and hydrogen to carbon
 702 within the leaves (closed circles), petioles (open circles), stems (closed triangle), stem
 703 cutting (open triangle) and roots (closed square). The circles overlain on the plots in
 704 (a) and (c) indicate atomic ratios characteristic for different compound classes
 705 (adapted from Sleighter & Hatcher, 2007). (a) illustrates the atomic ratio of all tissues
 706 measured (15 replicates \pm one standard deviation, (b) the isotopic ratios of the ^{13}C ,
 707 ^{18}O and ^2H excess atom fraction (relative to the unlabelled tissues) measured after
 708 equilibrium in the labelling (see Fig. 1 and 2) was reached ($t = 8$ and 14, six replicates
 709 \pm one standard deviation) and (c) shows the isotopic ratios of after normalization with
 710 the maximum label strength of the leaf water (^{18}O , ^2H) and water-soluble organic
 711 matter (^{13}C)



(1) Sampled after 3/12 hours daylight; errors represent variability between plant individuals (three plant replicates each sampling date).
 (2) Integrated value over 2-3 days (water trap analysed at day 6, 8, 11 and 14), errors represent variability between sampling date 8 and 14.
 (3) Average of all watering dates (day 0, 2, 6, 8, 11); errors represent variability between sampling dates.
 (4) Measured at the beginning of the experiment

713
 714 **Figure A1.** Overview on the input data of the two-source isotope mixing model. $\delta^{18}\text{O}$
 715 and $\delta^2\text{H}$ signatures of the water pools of the chamber system are presented as average
 716 values after equilibrium in the labelling was reached ($t = 8$ and 14 days). The
 717 monitored environmental conditions ($T =$ temperature, $a\text{H} =$ absolute humidity and $r\text{H} =$
 718 relative humidity) are presented in grey. The equilibrium and kinetic fractionation
 719 factors, highlighted in blue, were calculated according to Majoube (1971) and Cappa
 720 et al. (2003), respectively. The fractionation factors were used for the calculations
 721 (green box) of the signatures in the non-directly measured pools and the isotopic
 722 signatures of the evaporating and condensation source of the leaf water (red box). The
 723 equations are given for $\delta^{18}\text{O}$, but apply for $\delta^2\text{H}$ analogously. Please note that the data
 724 reported here are average values of the two last sampling dates, while we present in
 725 the result section the data of single sampling dates or average values of the whole
 726 labelling experiment (environmental conditions, equilibrium fractionation factors)

727 **Appendix B**

728 Calculation of the relative air humidity and the dew-point temperature

729 The dew-point temperature, i.e. the temperature at which the water condensed inside
 730 the peltier-cooled water condenser ($T_{\text{pelt,DP}}$) was calculated by solving Equation B1
 731 with the humidity measured in the air after the condenser ($10 \pm 1 \text{ mmol mol}^{-1}$ $a\text{H}$, 26
 732 % $r\text{H}$).

733
$$rH(T) = \frac{e}{e(T)} \cdot 100 \tag{B1}$$

734 , where rH is the relative air humidity (in %), e is the partial pressure of water vapour
735 (calculated according to Eq. B2) and e(T) is the saturation vapour pressure (in kPa,
736 calculated according to Eq. B3).

737
$$e = \frac{aH}{1000} \cdot p \tag{B2}$$

738 , where aH is the absolute humidity given as the mole fraction of water vapour (mmol
739 mol⁻¹) and p is the atmospheric pressure (in kPa).

740
$$e(T) = 0.61365 \cdot e^{\frac{17.502 \cdot T}{240.97 + T}} \tag{B3}$$

741 , where T is the room air temperature (in °C).

742 References

743 Cappa C.D., Hendricks M.B., Depaolo D.J. and Cohen R.C.: Isotopic fractionation of
744 water during evaporation. J Geophys. Res., 108,: 4525. doi: 10.1029/2003
745 JD003597, 2003.

746 Majoube M.: Fractionnement en oxygène 18 et en deutérium entre l'eau et sa vapeur.
747 J. Chim. Phys. physico-chimie Biol., 68,1423–1435. 1971.

748